

# Determination of Lithology, Porosity and Water Saturation for Mishrif Carbonate Formation

F. S. Kadhim, A. Samsuri, H. Alwan

**Abstract**—Well logging records can help to answer many questions from a wide range of special interested information and basic petrophysical properties to formation evaluation of oil and gas reservoirs. The accurate calculations of porosity in carbonate reservoirs are the most challenging aspects of the well logging analysis. Many equations have been developed over the years based on known physical principles or on empirically derived relationships, which are used to calculate porosity, estimate lithology, and water saturation; however these parameters are calculated from well logs by using modern technique in a current study. Nasiriya oil field is one of the giant oilfields in the Middle East, and the formation under study is the Mishrif carbonate formation which is the shallowest hydrocarbon bearing zone in this oilfield. Neurolog software was used to digitize the scanned copies of the available logs. Environmental corrections had been made as per Schlumberger charts 2005, which supplied in the Interactive Petrophysics software. Three saturation models have been used to calculate water saturation of carbonate formations, which are simple Archie equation, Dual water model, and Indonesia model. Results indicate that the Mishrif formation consists mainly of limestone, some dolomite, and shale. The porosity interpretation shows that the logging tools have a good quality after making the environmental corrections. The average formation water saturation for Mishrif formation is around 0.4-0.6. This study is provided accurate behavior of petrophysical properties with depth for this formation by using modern software.

**Keywords**—Lithology, Porosity, Water Saturation, Carbonate Formation, Mishrif Formation.

## I. INTRODUCTION

GIVEN knowledge of the rock type, porosity can be determined by using different logging devices. For example, if a density logging tool is to be used, the rock matrix density must be known in order to determine the porosity. Likewise, using sonic log for porosity determination, the known parameter must be the matrix travel time and for neutron log, the parameter that must correspond to the rock type is the matrix setting for the neutron logging tool. If the encountered lithologies are simple or if the detailed information about the geology of the formation is shown, many problems should not arise in the determination of these parameters. Otherwise, the best way is to adopt the graphical methods if lithology is uncertain.

Fluid flow through heterogeneous carbonate reservoirs

F.S. Kadhi is with the Department of Petroleum Engineering, Faculty of Petroleum and Renewable Energy, Universiti Teknologi Malaysia, 81310, Skudai, Johor, Malaysia (e-mail: skfadhil2@live.utm.my).

A. Samsuri is with the Department of Petroleum Engineering, Faculty of Petroleum and Renewable Energy, Universiti Teknologi Malaysia, 81310, Skudai, Johor, Malaysia.

H. Alwan is with the Iraqi Drilling Company, Basrah, Iraq.

(limestone and dolomite) is a substantially different process from the flow through the homogeneous sandstone reservoir. This variation is largely caused by the fact that carbonate rocks tend to have a more complex pore system than sandstone [1], [2]. In the Middle East, Carbonate reservoirs are very heterogeneous in terms of rock types. Therefore, the reservoir should be split into layers on the basis of the dominant rock type in order to define average values and trends of petrophysical parameters in the reservoir rocks [3].

A Cross plot of porosity logging data has been in use since early 1960 [4]. Today an extremely large variety of two and three-dimensional cross-plots are available. There are many cross-plots models can be used for each formation to determine the lithological type, such as mono, binary and triple-mineral. Assuming a reservoir rock of known lithology, which is clean and /or shale corrected, then each porosity value can be explained for cross-plots type [5].

The density-sonic cross plot is the first cross-plot. As water-filled porosity increases, three different loci could be traced out for differing travel times and matrix densities for the three principal matrices. A considerable confusion in the ascribed lithology caused by a little uncertainty in the measured pair ( $\Delta_r$ - $\text{Rho}_B$ ) means the contrast between the matrix endpoints is not a great deal. In addition, depending on the type of sonic transform used, there is a large difference as well [6], [7].

The density log is a continuous record of a formation's bulk density. It is used mainly for the determination of porosity, and the differentiation between liquids and gasses (when used in combination with neutron log). When organic content is present, density is low. Variation of density indicates porosity changes. For example, low density indicates high porosity [8]. The second one is the combination cross-plot between neutron and sonic logs. For a thermal neutron porosity device, the travel times as a function of the apparent porosity are plotted. A considerable separation between limestone, dolomite, and sandstone appears due to the matrix effect of the neutron device [6].

One of the most controversial problems in the formation evaluation is the clay effect to reservoir rocks [9]. Shale is usually more radioactive than sand or carbonate, the gamma ray log and other logs can be used to calculate the volume of shale in a porous medium. The volume of shale expressed as a decimal fraction or percentage is called shale volume ( $V_{\text{shale}}$ ) [10]. The volume of clay can be calculated by two sets of well-logging indicators that are Single Clay Indicators and Double Clay Indicators; the minimum value of clay ( $V_{\text{clay}}$ ) is the closest to the truth [11], [12].

There is always more than one fluid phase occupying the

pore space in a petroleum and gas reservoirs. The fluid saturation is the petrophysical property that describes the amount of each fluid type in the pore space. It is defined as the fraction of the pore space ( $V_p$ ) occupied by a fluid phase ( $V_F$ ) as:

$$\text{Saturation} = \frac{V_F}{V_p} \quad (1)$$

One of the most troublesome aspects of log analysis is the calculation of water saturation ( $S_w$ ). There are many equations, and empirical correlations have been developed over the years to calculate the ( $S_{wi}$ ). Resistivity and Conductivity are common methods to calculate water saturation. In the earliest days of well-logging resistivity logs are the most commonly used measurements to determine ( $S_w$ ). A high resistivity log reading in a porous medium can be indicated by the presence of hydrocarbon [13], [14]. While the principle of conductivity method depend on sodium cations concentration, that can be calculated in term of Cation Exchange Capacity (CEC), expressed in mille equivalents per gram of dry clay.

The field of study is located in the north of Arabian platform in the Middle East between latitudes (34°80' - 34°60' N) and longitudes (57°50' - 60°10' E). It is anticline structure with northwest- southeast general trend. Three reservoir units contain most of the oil within the reservoir; the Yamamma, Nahr Umr, and Mishrif formations [15]. Mishrif formation is divided into two main reservoir units: the Upper Mishrif and the Lower Mishrif which consist mainly of limestone. This formation is an important reservoir unit due to rudist deposits [16], [17].

In this study, the lithology, Porosity, and water saturation of Mishrif formation were determined using corrected well log data and compared with core data that obtained from NS-3 well [18]. The accurate determination the saturation values with depth will improve the oil in place calculation and consequently detected the perforation zones.

## II. METHODOLOGY

Cross-plot techniques are employed in the analysis of well logging data. A set of log data from the NS field was used as the base data for the research reported in this paper. Neura-Log software V 2008.5 was used to digitize the scanned copies of logs in which the results as LAS files were loaded into the Interactive Petrophysics software (IP) where the reading measurements were taken as one reading per 0.1524 meters. The log curves are checked to be for depth with each other.

Environmental corrections were made using the current Schlumberger charts (SLB, 2005) for available logs (gamma ray (Gr), resistivity logs (ILD and MSFL), density log (RHOB) and neutron log (NPHI). These charts are supplied to IP as the environmental correction module. Actual mud properties, caliper log, hydrostatic pressure and temperature gradient were provided for accurate corrections. Depending on well logging data the Interactive Petrophysics software (IP V3.5, 2008) had been used to calculate the porosities and

determine the lithology cross-plots.

## III. RESULTS AND DISCUSSION

### A. Porosity

Formation density log, sonic log or neutron log all, can determine the values of porosity. Other parameters such as the nature of the fluid in pore spaces, lithology and shaliness also have effects on those logs also to porosity. Generally, a combination of logs is used to obtain more accurate porosity values. The properties of the formation close to the borehole determine the readings of the tools. The shallowest investigation is carried out with a sonic log. Generally, within the flushed zone, neutron and density logs are affected by a little deeper region depending somewhat on the porosity.

The density tool responds to the electron density of the material in the formation. Formation bulk density ( $Roh_B$ ) is a function of matrix density, porosity, and density of fluids in the pores (salt water, fresh water mud, or hydrocarbons). The formula for calculating density-derived porosity is [6], [9]:

$$\text{PhiDen} = \Phi_D = \frac{2.71 - Roh_B}{2.71 - Roh_f} \quad (2)$$

where:  $Roh_B$ : is the bulk (matrix) density, [2.71 (gm/cc) for limestone, 2.87 (gm/cc) for dolomite and 2.65 (gm/cc) for sandstone].  $Roh_f$ : is the fluid density (gm/cc) [fresh water mud = 1, for salt water mud 1.1].

The neutron log (NPHI) is used mainly for lithology identification, porosity evaluation, and the differentiation between liquids and gasses when used in combination with density log. On cross-plot of neutron and density logs, pure shale can be recognized by the high neutron value relative to the density value which gives a large positive separation to the logs while gas stands out distinctly giving a large negative separation [8].

Neutron logs are porosity logs that measure the hydrogen concentration in a formation. In clean formations (shale-free), where the pores are filled with water or oil, therefore, hydrogen is concentrated in the fluid-filled pores, energy loss can be related to the formation porosity. Whenever shale is part of the formation matrix, the reported neutron porosity is greater than the actual formation porosity [10].

The sonic log is a porosity log that measures interval transit time ( $\Delta t$ ) of a compressional sound wave traveling through the formation; the interval transit time depends on both lithology and porosity. Wyllie time-average equation may be written as [19]:

$$\text{PhiSon} = \Phi_S = \frac{\Delta t_{\log} - \Delta t_{mat}}{\Delta t_f - \Delta t_{mat}} \quad (3)$$

where:  $\Phi_S$  is sonic-derived porosity, fraction,  $\Delta t_{ma}$ : is the interval transit time in the matrix [Its value is 47.6  $\mu\text{sec}/\text{ft}$  for limestone and 43.5  $\mu\text{sec}/\text{ft}$ , for dolomite],  $\Delta t_{\log}$ : is the interval transit time in the formation,  $\mu\text{sec}/\text{ft}$ .,  $\Delta t_f$ : is the interval transit time in the fluid within the formation [For freshwater mud =

189 ( $\mu\text{sec}/\text{ft}$ ); for salt-water mud = 185( $\mu\text{sec}/\text{ft}$ ).

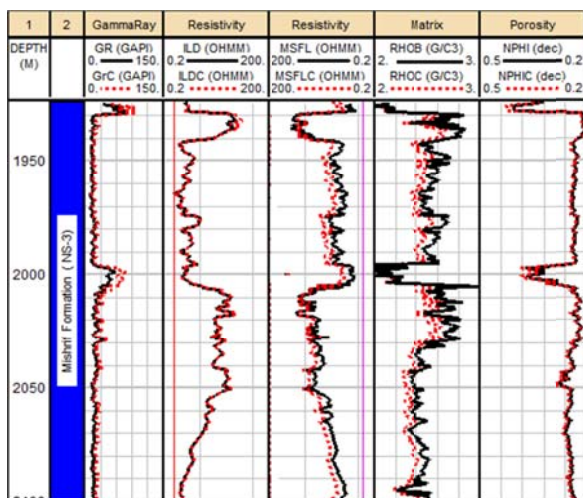


Fig. 1 Environmental correction of well logs

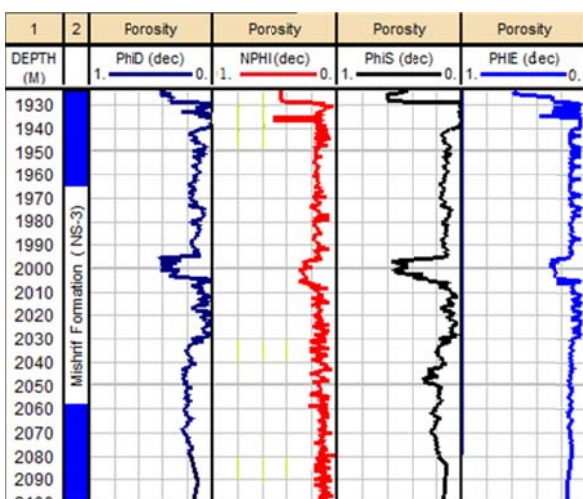


Fig. 2 Porosity results

TABLE I  
 COMPARISON RESULT OF CORE - LOG AVERAGE POROSITY

Core no.	Depth Interval (m)	$\Phi_{\text{CORE}}$	$\Phi_{\text{CPI}}$
C1	1991.98-2005.30	0.113	0.112
C2	2005.97-2018.50	0.123	0.102
C3	2019.58-2025.50	0.154	0.139
C4	2039.40-2042.00	0.223	0.207
C5	2057.40-2073.90	0.223	0.220

Using IP software, corrections were achieved per 0.1524 m of depth to avoid erroneous results in water saturation interpretations. The software supplied the correction charts (SLB, 2005) as the environmental correction module. The environmental corrected and porosity results of well logs are shown in Figs. 1 and 2. The Computer-Processed Interpretation (CPI) results of effective porosity ( $\Phi_{\text{CPI}}$ ) are closed to the core porosity ( $\Phi_{\text{CORE}}$ ) as shown in Table I and Figs. 3-6 that means the porosity interpretation by porosity logging tools have good quality after making the environmental correction. The relationship between core and

CPI porosity is shown in Fig. 7. From this figure, the corrected equation for effective porosity was produced. This equation was used to correct the CPI value of the effective porosity as shown in Fig. 8. The main reason that leads to differences between the porosity value from core and log is the varying between properties of formation water and the mud filtrate [20]. The Ferro Chrome Lignite - Chrome Lignite (FCL-CL) was used as drilling mud in the NS-3 well [18]. The (FCL-CL) mud contains barite as a weighting agent and characterized by a high ratio of free phase (water), which lead to a high diameter of invasion zone (more than 50 in), that mean barite invaded the investigation zone for logging tools.

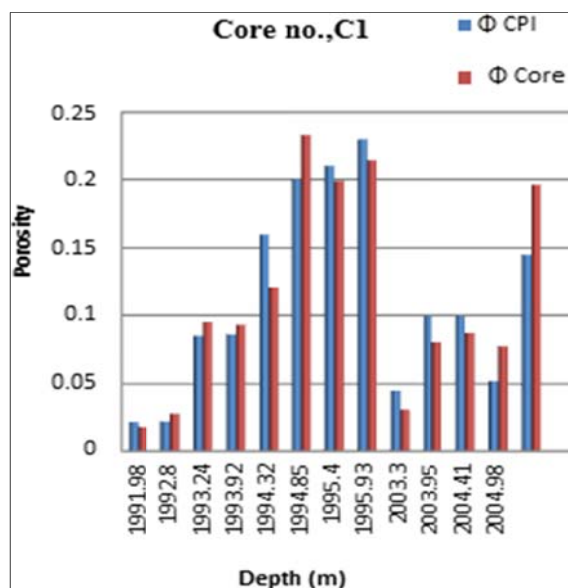


Fig. 3 Comparison between core and CPI porosity results for C1

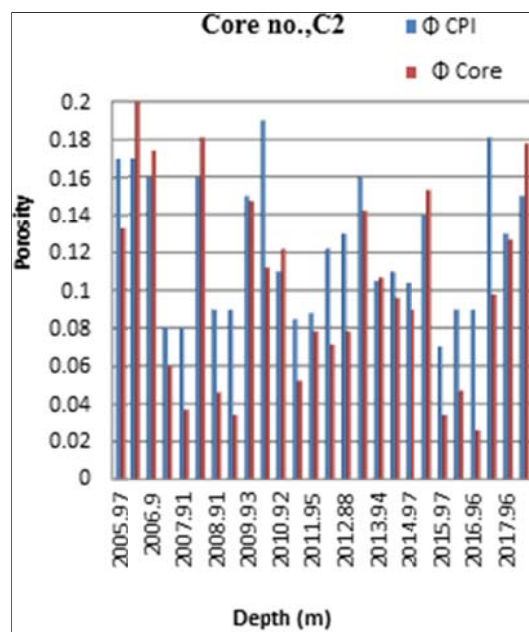


Fig. 4 Comparison between core and CPI porosity results for C2

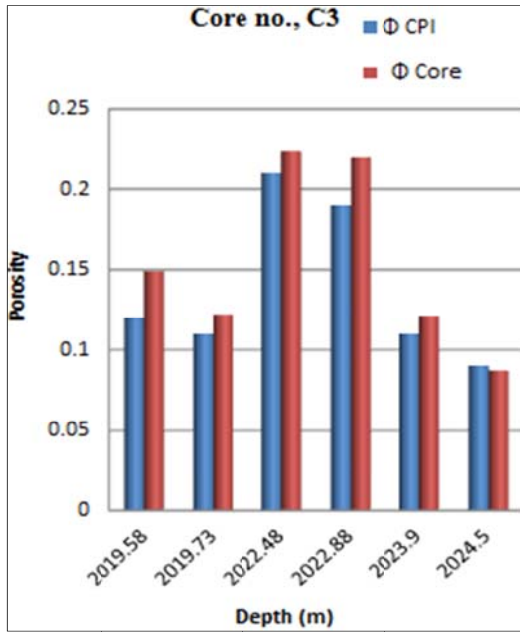


Fig. 5 Comparison between core and CPI porosity results for C3

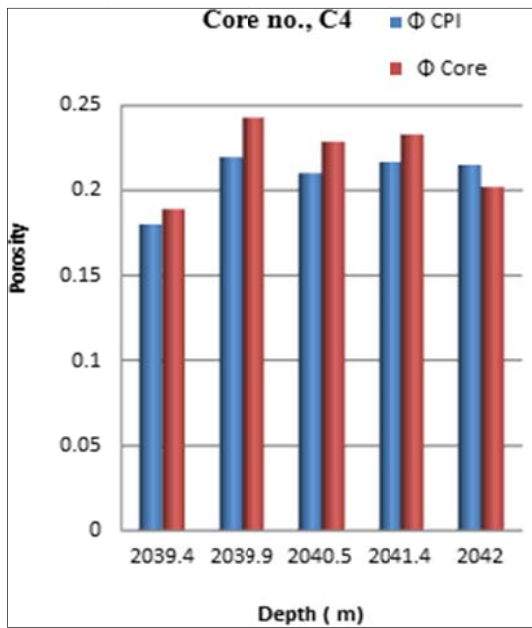


Fig. 6 Comparison between core and CPI porosity results for C4

**B. Lithology**

By virtue of the different responses of matrix minerals to the individual porosity logs, immediate indications of the lithology of logged units will be given by an overlay of any combination of the three porosities. The hypothetical response to a mixed sequence of lithologies can be compared to the density, sonic, and neutron logs to illustrate this point.

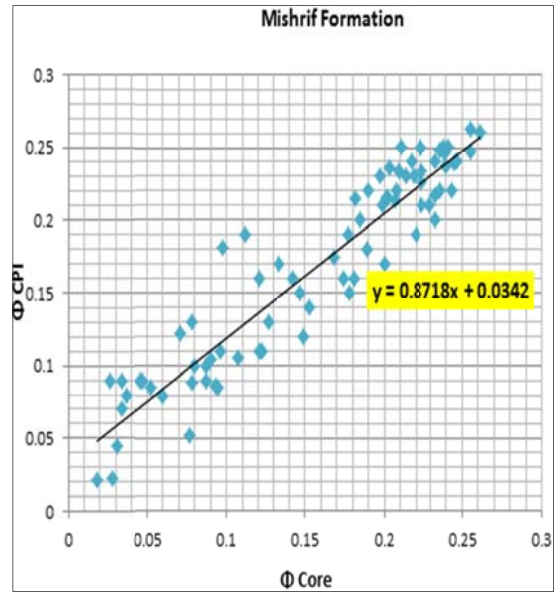


Fig. 7 ΦCPI and ΦCore relationship

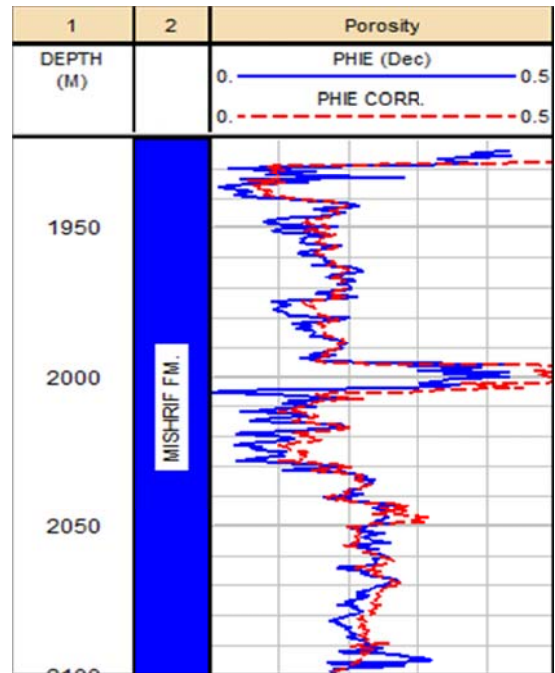


Fig. 8 Effective porosity results as per core correction equation

A cross-plot of two porosity logs is convenient to display both porosity and lithology information. This cross-plot was constructed for clean, liquid saturated formation and boreholes filled with water or water-based mud. The sonic-neutron cross-plot for Mishrif Formation is shown in Fig. 9, which illustrates the separation between the sandstone, limestone and dolomite lines that indicate a good resolution for these lithologies. Fig. 9 illustrates sonic-neutron cross-plot for Mishrif Formation, which provides a resolution between sandstone, limestone, anhydrite and dolomite lithologies. No secondary porosity effects were noticed since both logs measure total porosity. The clay effect is clearly noticed by



shifting some points towards the east, and the bad hole effects make some points to be scattered. The lithology results are quite similar with [16] and [17], descriptions of Mishrif formation lithology.

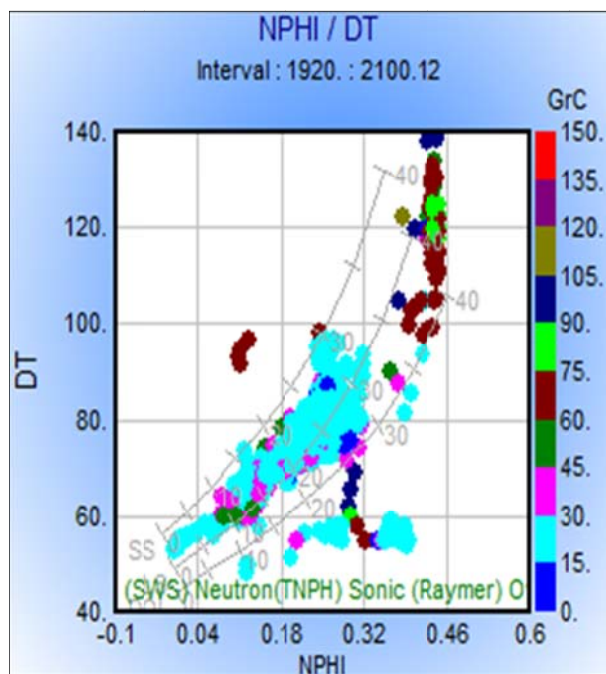


Fig. 9 Interval transit time (DT) vs. Neutron Porosity (NPHI) cross plot

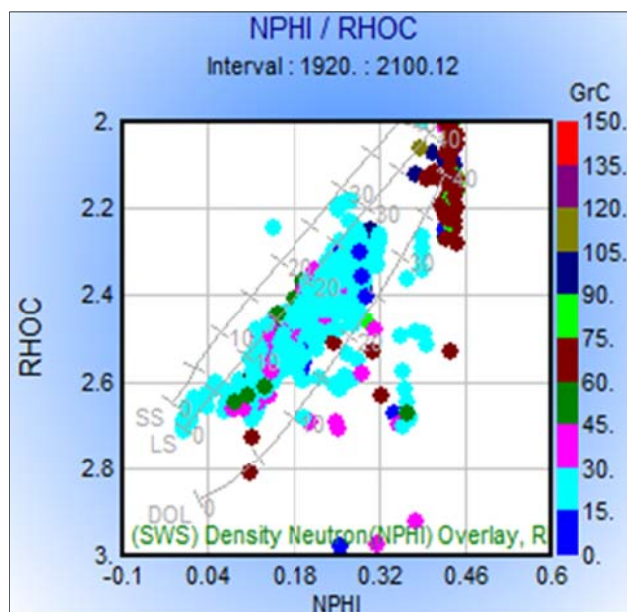


Fig. 10 Corrected Bulk density (RHOC) vs. Neutron porosity (NPHI) cross plot

As in the previous cross-plot the density-neutron cross plot is provided for clean fully liquid-saturated formations and holes filled with water or water based mud. Fig. 10 shows the density-neutron cross-plot for Mishrif Formation. The density-

neutron cross-plot provides a satisfactory resolution of porosity and lithological column. Here too, no secondary porosity effects were noticed for the same reason stated above. Also, the clay effect is clearly noticed by shifting some points towards the east, and the bad hole effects make some points to be scattered, as shown in Fig. 9.

### C. Clay Volume

The spectral gamma ray (SGR) provides the measure of the total natural radioactivity of the formation. The spectral gamma ray tool detects the naturally occurring gamma rays and defines the energy spectrum of the radiations. Because Potassium (K), Thorium (Th) and Uranium (UR) are responsible for the energy spectrum observed by the tool, their respective elemental concentrations can be calculated [12]:

$$V_{clay} \leq \frac{SGR - SGR_{min}}{SGR_{max} - SGR_{min}} \quad (4)$$

$$(V_{clay})_{UR} \leq \frac{UR - UR_{min}}{UR_{max} - UR_{min}} \quad (5)$$

$$(V_{clay})_K \leq \frac{K - K_{min}}{K_{max} - K_{min}} \quad (6)$$

$$(V_{clay})_{Th} \leq \frac{Th - Th_{min}}{Th_{max} - Th_{min}} \quad (7)$$

Since the Uranium is associated with radioactive minerals other than those found in clay (i.e. Organic materials), so it is not a reliable clay indicator. By eliminating the uranium contribution from the total gamma ray response and defining the Corrected Gamma Ray CGR (i.e., sum of thorium and potassium only) [12]:

$$V_{sh} \leq \left[ \frac{CGR - CGR_{min}}{CGR_{max} - CGR_{min}} \right] \quad (8)$$

where: CGR: Corrected gamma ray logs reading in the zone of interest (API units),  $CGR_{min}$ : Corrected gamma ray logs reading in a 100 % clean zone (API units),  $CGR_{max}$ : Corrected gamma ray logs reading in 100% shale (API units).

Neutron log reading provides an equation that often used to calculate the shale volume [12], [21].

$$V_{sh} = \sqrt{\left( \frac{\Phi_N}{\Phi_{Nclay}} \right) \left( \frac{\Phi_N - \Phi_{Nclay}}{\Phi_{Nclay} - \Phi_{Nclean}} \right)} \quad (9)$$

The resistivity of a mixture of clay with some non – conductive mineral (quartz for example) will depend on clay resistivity and clay content. If the mixture has no porosity, then it can be expressed by an Archie – type formula [12], [21]:

$$R_t \leq \frac{R_{clay}}{(V_{clay})^b} \quad (10)$$

In case of low porosity, some formation water will exist, and so the resistivity will be lower also, therefore:

$$V_{sh} \leq \left( \frac{R_t}{R_{clay}} \right)^{1/b} \quad (11)$$

The above equation is used in case of high to moderated values of porosities, but in general form the following formula will use [12]:

$$V_{sh} \leq \left[ \frac{R_{clay} (R_{max} - R_t)}{R_t (R_{max} - R_{clay})} \right]^{1/b} \quad (12)$$

where:  $R_{max}$  is the maximum resistivity reading in the clean hydrocarbon bearing interval,  $1/b$  is equal to one when  $(R_t/R_{clay}) \geq 0.5$  or equal to  $\{0.5 / (1 - R_t/R_{clay})\}$  when  $R_t/R_{clay} < 0.5$ . The clay volume results are shown as follows in Fig. 11

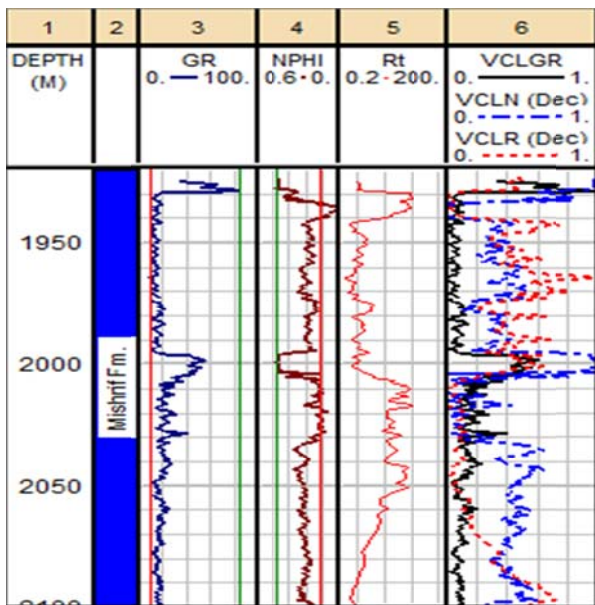


Fig. 11 Clay Volume Results

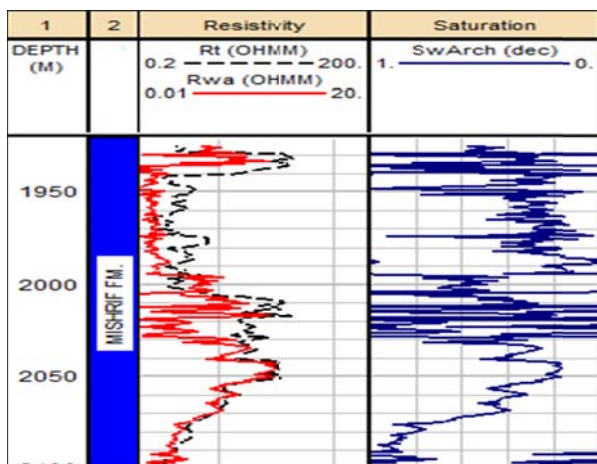


Fig. 12 Water Saturation Results of Archie Model

#### D. Water Saturation

Archie in 1942 was introduced equation, which based on laboratory experiments on clean sands, water wettability and non-vugy carbonates. The earliest research established that for a formation with constant porosity and water salinity, an increase in resistivity indicated the presence of hydrocarbons. Archie qualified this relationship as shown in [20], [22]:

$$S_w^n = \frac{a \cdot R_w}{R_t \cdot \Phi^m} \quad (13)$$

The results of Archie's model are shown in Fig. 12.

In 1971 Poupon and Leveaux introduced Indonesia model. This model was derived based on the fresh waters saturation and clay volume that present in many oil reservoirs in Indonesia. Conductivities of the shale and formation water are affected by the relationship between true resistivity and water saturation in this model. The Indonesia formula can be written as [20]:

$$S_w^{0.5} = (R_t)^{-0.5} \left[ \frac{V_{cl}^d}{R_{cl}^{0.5}} + \frac{\Phi^{0.5m}}{(aR_w)^{0.5}} \right] \quad (14)$$

where:  $d=1-0.5 V_{cl}$ . Indonesia model results are shown in Fig. 13, track number three.

Conductivity models are improved the water saturation results by matching well log data with laboratory measurements. The most commonly used cation exchange capacity model is a dual water model. The dual water model is modified from Waxman-Smits model by calculation the conductivity of free water away from clay surface and the relative volume of clay bound water for double-layer. This model is given by two types of formation water as follows [23], [24]:

- A. Bound Water Saturation  $S_{wB}$ , which defined as the fraction of total porosity occupied by bound water.
- B. Free Water Saturation  $S_{wF}$ , which defined as the fraction of total porosity occupied by free water.

$$S_{wT} = Y + \left[ \frac{R_{wT}}{\Phi_T^2 R_t} + Y^2 \right]^{1/2} \quad (15)$$

where:

$$Y = \frac{S_{wB} (R_{wB} - R_{wF})}{2R_{wB}} \quad (16)$$

and;  $R_{wT}$  is a resistivity of free water,  $S_{wT}$  is total water saturation,  $R_{wB}$  is a resistivity of bound water. The Dual-Water model results are shown in Fig. 13 in the track four.

Table II shows the results of water saturation from Archie, Indonesia, dual- water models and core saturation. Archie formula gives a misleading result that is because it assumes that the formation water is the only electrically conductive material in the formation, which is not true for the case of shale formation. The shale effect on various log responses

depends on the type, the amount, and the way is distributed in formation [8].

Universiti Teknologi Malaysia (UTM) for supporting a research assistantship.

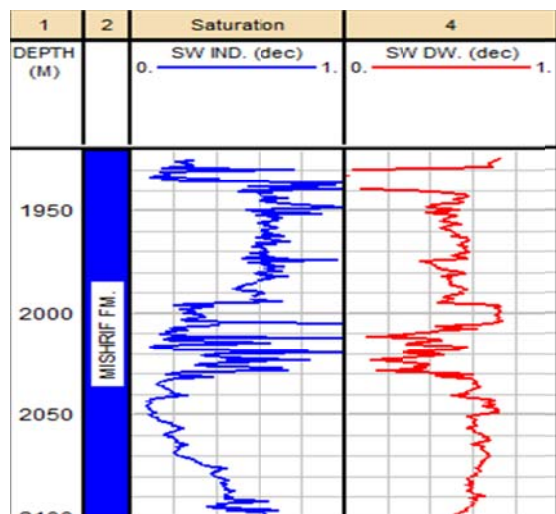


Fig. 13 Water Saturation Results of Indonesia and Dual-Water Model

In shale formations, it is accepted that the Dual water conductivity model which using total porosity gives water saturation results that are more consistent than resistivity type equations [20]. However the conductivity models have inherent problem which is the total porosity cannot be measured without calibration with core analysis since the dry clay matrix points do not exist in nature and is therefore not seen by the logs.

TABLE II  
WATER SATURATION RESULTS FROM LOGS AND CORE

Level	Depth interval (m)	Sw Arch.	Sw IND	Sw DW	Sw Core
Mb-1	2007-2030	0.53	0.55	0.40	0.51
Mb-2a	2030-2081	0.52	0.30	0.62	0.50
Mb-2b	2081-2097	0.94	0.57	0.60	0.93

#### IV. CONCLUSIONS

The major findings of the current study can be summarized as:

1. Cross-plots interpretations show that the Mishrif reservoir consists mainly of limestone, some dolomite, and shale.
2. The environmental correction for sonic, density and neutron logs gives accurate values of porosity and the average effective porosity for Mishrif formation is almost between 0.1-0.22
3. The results show the effect of clay while there is no secondary porosity effect.
4. The Dual water model gives water saturation results that are more consistent than resistivity type equations and the average water saturation value for Mishrif formation is located between 0.4-0.6.

#### ACKNOWLEDGMENT

The authors would like to thank the Ministry of Higher Education (MOHE) in Iraq for providing a research grant and

#### REFERENCES

- [1] G. V. Chilingar, H. G. Bissell, K. H., Wolf. 1979. *Diagenesis of Carbonate sediments and epigenesis (or catagenesis) of limestone*, Larsen, G., and Chilingar, G. V. (Editors), *Diagenesis in Sediments and sedimentary rocks, developments, in sedimentology*. 25 A. Elsevier, Amsterdam, Pp 247-422.
- [2] S.J. Mazzullo. 1986. *Stratigraphic approach of hydrocarbon exploration and exploitation*. Geol. J., 21:265-28.
- [3] F. S. Kadhim, S. Samsuri, A. Idris. 2013, A review in correlation between cementation factor and carbonate rock properties, *Life Sci. J*, 10(4):2451-2458
- [4] R. M. Bateman, C. E. Konen. 1977. *The Log Analyst and the Programmable Pocket Calculator, Part II: Cross-plot Porosity and Water Saturation*, Society of Petro physicists and Well Log Analysts, SPWLA-Vx-No.6.
- [5] J. A. Burke, R. L. Campbell, A. w. Schmidt. 1969. *The Litho-Porosity Crossplot SPE*, 2547.
- [6] V. E. Darwin, M. s. Julian. 2007. *Well Logging for Earth Scientists*, 2<sup>nd</sup> Edition, Springer, pp 629-634
- [7] Schlumberger. 1989. *Log Interpretation Principles / Applications*, Eight Printing, Sugar Land, Texas
- [8] O.C Akinyokun, P.A. Enikanselu, AdeyemoA.B., A. Adesida., 2009. Well Log Interpretation Model for the Determination of Lithology and Fluid Contents, the *Pacific Journal of Science and Technology*, 10 (1): 507-517.
- [9] G.M Hamada 1999. An Integrated Approach to Determine Shale Volume and Hydrocarbon Potential in Shaly Sand in the Gulf of Suez, Society of Petro physicists and Well Log Analysts, SPWLA-V40, No3
- [10] A. Asquith, D. Krygowski. 2004. *Basic Well Log Analysis*. The American Association of Petroleum Geologists Tulsa, Oklahoma.
- [11] L. M. Susan, R. S. Robert. 1990. *The effect of Lithology, Porosity and Shaliness on P-Wave and S-Wave Velocities from Sonic Log*, Canadian Journal of Exploration Geophysics, Vol.26: 94-103.
- [12] Schlumberger, 2008. *The IP Interactive Petrophysics, V-3.5, Manual*.
- [13] P.D. Jackson, J.F. Williams, M.A. Lovell, A. Camps, C Rochelle, A.E. Milodowski. 2008. *An Investigation of The Exponent in Archie's Equation: Comparing Numerical Modeling with Laboratory Data towards Characterizing Disturbed Samples from the Cascadia Margin, The 49th Annual Logging Symposium, 25-28 May, Austin, Texas, SPWLA-2008- HHH*.
- [14] L Adeoti, E.A. Ayolabi, P.L. James.2009. *An Integrated Approach to Volume of Shale Analysis: Niger Delta Example, Orire Field*, The World Applied Sciences Journal, 7 (4): 448- 452.
- [15] M.H. Amnah. 2009. *Prediction of Reservoir Permeability from well Logs Data Using Artificial Neural Networks*, *Iraqi Journal of Science*. 50(1):67 – 74.
- [16] S.Z. Jassim, J.C. Goff. 2006. *Geology of Iraq*, Dolin, Prague and Moravian Museum Brno., Pp.341
- [17] A. A. Aqrabi, G.A. Thehni, G. H. Sherwani, B. M. Kareem 1998, Mid-cretaceous rudist-bearing carbonate of the Mishrif formation: An important reservoir sequence in the Mesopotamian basin, *Iraqi Journal of Petroleum Geology*, 21(1): 57-8
- [18] Iraqi National Oil Company. 1985. NS-3 Unpublished Final Well Report.
- [19] L.M. Etnyre. 1989. *Finding Oil and Gas from Well Logs*. Van Nostrand Reinhold, New York. Pp 21-25.
- [20] A.T Amin, M. Watfa, M. A. Awad. 1987. *Accurate estimation of Water saturation in complex carbonate reservoir*, SPE-15714MS: Society of Petroleum Engineers presented at the 5<sup>th</sup> SPE Middle East Oil show in Bahrain, p.16
- [21] E.C. Thomas, S.J. Stieber. 1975. *The Distribution of Shale in Sandstones and Its Effect upon Porosity*, the 16th Annual Logging Orleans, Symposium, June 4-7, New Orleans, Louisiana, SPWLA- 1975-T
- [22] G. E. Archie. 1942. *The Theoretical Resistivity Log as an Aid in Determining Some Reservoir Characteristics* SPE-942054-G.
- [23] G. Coates, Y. Boutemy, C. Clavier, C.1983. *A Study of the Dual-Water Model Based on Log Data*, SPE 10104-PA.
- [24] C. Clavier, G. Coates, J. Dumanior.1984. *Theoretical and Experimental Bases for the Dual-Water Model for Interpretation of Shaly Sands*, SPE 6859-PA: 1153-168.